CHAPTER 17

SINGLE AND TWO-PHASE FLOW DIAGNOSTICS AND MONITORING

W.J.G. Brimley
Process Systems Development
Atomic Energy of Canada - Engineering Company
Mississauga, Ontario

Jen-Shih Chang
Dept. Engineering Physics and M.I.E.S.
McMaster University
Hamilton, Ontario

ABSTRACT

Instrumentation used for single and two-phase flow measurements is briefly discussed. Devices used to measure temperature, pressure, flow, liquid level, quality, and void fraction are presented. Applications of these devices to CANDU reactors are described.

17.1 Introduction

In the primary heat transport system of existing CANDU reactors, pressures, temperatures and flow are monitored.

Capacitance-type pressure transmitters are used to measure absolute and differential pressures. Typical absolute pressure measurements are taken at the pressurizer, reactor outlet headers (ROH), pump suction, and reactor inlet headers (RIH). Typical differential pressures are recorded across the headers (ROH-ROH, RIH-ROH), and the pump ΔP is recorded.

RTD's are mounted in thermowells which are immersed into the headers or strapped onto feeders. Pressurizer, RIH and ROH temperatures are measured, and all outlet feeder temperatures are measured (380 temperatures in 600 MW reactor). RIH to ROH differential temperatures are also monitored.

Single phase flows are measured in the instrumented channels (12 channels in 600 MW reactor) by measurements of differential pressures across orifice plates permanently installed in inlet feeders. The differential pressures are recorded by a capacitance-type pressure transmitter.

During cold commissioning, temporary ultrasonic flowmeters have been used to measure all the channel flows and shut down cooling flows. As a result pump gross flows can be determined. Also, the instrumented channels with flows measured simultaneously by ultrasonic flowmeters and the permanent orifice meters allows a valuable check on the measurements.

Copyright M.I.E.S. 1982

Advanced instrumentation such as void fraction, liquid film thickness, acoustic emission techniques which would be used in future CANDU related diagnostics are also outlined.

17.2 TEMPERATURE

A basic list of devices to measure temperature includes:

thermometers
thermocouples
RTD's (Resistance Temperature Detectors)
thermistors (semiconductor sensors)
radiation detectors (optical, radiation pyrometers).

However the two devices used almost exclusively for temperature measurements in CANDU reactors and related laboratory experiments are thermocouples and RTD's.

17.2.1 Thermocouples

If wires of different materials are joined and subjected to a temperature gradient, a net EMF can be generated. An equation describing this may be written as:[1]

$$E_{NET} = \int_{T_1}^{T_2} E_1 \, dT + \int_{T_2}^{T_1} E_2 \, dT$$

where E_1 and E_2 represent the absolute values of the EMF's of the two metals 1 and 2, respectively.

It should be noted that the net EMF is the sum of the EMF's generated in each individual wire, and only those portions of the wires experiencing a temperature gradient affect the EMF.

Thermocouples when properly calibrated can be very accurate (e.g. Type E Platinum/platinum-rhodium error $\pm$0.25% of reading), and Table 1[2] gives the ANSI standard for thermocouple error limits. Figure 1[2] is a temperature-millivolt graph of the thermocouple types, and the curves also show the temperature ranges that the various thermocouple types can tolerate. As expected the most accurate type E thermocouple has the largest slope of millivolt output to temperature change, and is fairly linear.

For precise work a good reference junction constant temperature is required, and most often an ice point (ice bath, or electronic) reference junction (0°C) is used, however hot junctions, and even ambient junctions may be used and the net EMF corrected by adding the reference junction voltage.

Relative advantages of thermocouples are their low cost, simplicity, and generally rapid response. Thermocouple construction can range from bare wires through sheathed (grounded or ungrounded) thermocouples, foil thermocouples, and thermocouples with radiation shielding

Copyright M.I.E.S. 1982

TABLE I ANSI LIMITS OF ERROR OF THERMOCOUPLES
ANSI Standard C96.1

ANSI TYPE	TEMPERATURE RANGE, °F.	LIMITS OF ERROR	
		STANDARD	SPECIAL
J	32 to 530	±4°F	±2°F
	530 to 1400	±3/4 %	±3/8 %
K	32 to 530	±4°F	±2°F
	530 to 2300	±3/4 %	±3/8 %
T	−300 to −75	–	±1 %
	−150 to −75	±2 %	±1 %
	−75 to 200	±1−1/2°F	±3/4°F
	200 to 700	±3/4 %	±3/8 %
E	32 to 600	±3°F	±2−1/4°F
	600 to 1600	±1/2 %	±3/8%
S,R	32 to 1000	±2−1/2°F	±2.5°F
	1000 to 2700	±1/4%	±1/4 %*
B	1600 to 3100	±1/2%	

TEMPERATURE-MILLIVOLT GRAPH FOR THERMOCOUPLES

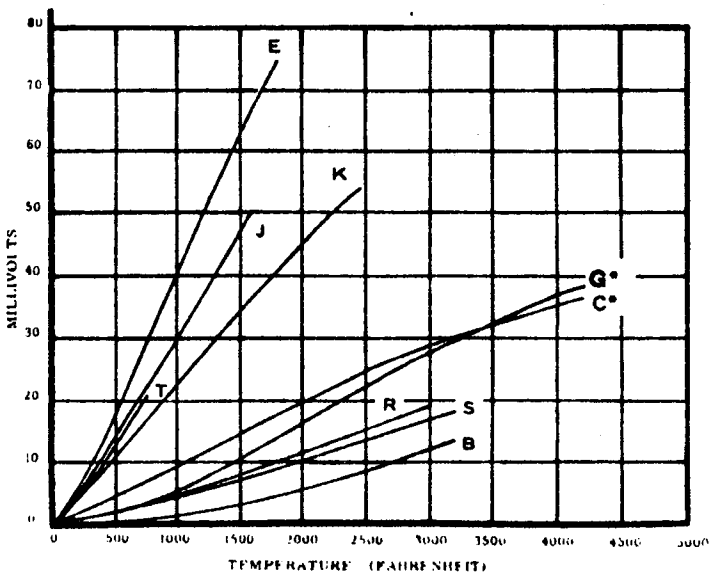

T	Copper vs. Constantan
E	Chromel vs. Constantan
J	Iron vs. Constantan
K	Chromel vs. Alumel
G*	Tungsten vs. Tungsten 26% Rhenium
C*	Tungsten 5% Rhenium vs. Tungsten 26% Rhenium
R	Platinum vs. Platinum 13% Rhodium
S	Platinum vs. Platinum 10% Rhodium
B	Platinum 6% Rhodium vs. Platinum 30% Rhodium

*Not ANSI Symbol

FIGURE 1

COMPARISON OF TIME CONSTANT* VS OVERALL OUTSIDE DIAMETER OF BARE THERMOCOUPLE WIRES OR GROUNDED JUNCTION THERMOCOUPLES

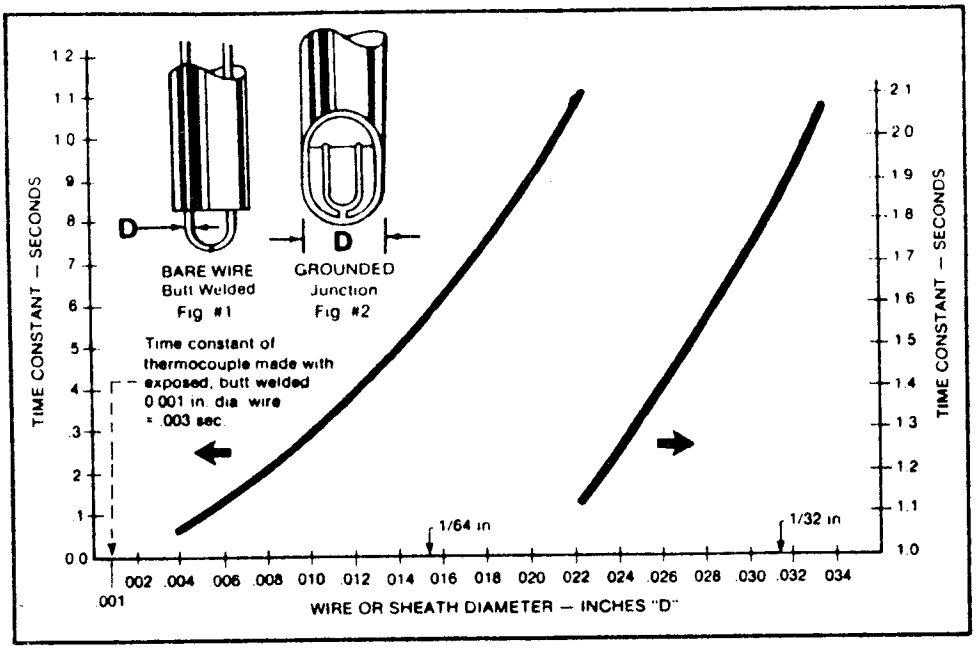

Time constants calculated for air at room temperature and atmospheric pressure moving with velocity of 65 feet per second for thermocouples shown in Figures #1 and #2.

For beaded-type and ungrounded junctions (Figures #3 or #4) multiply time constants by 1.5.

Time constant of thermocouple made with exposed butt welded 0.001 inch dia. wire = .003 sec.

* The "Time Constant" or "Response Time" is defined as the time required to reach 63.2% of an instantaneous temperature change.

Because of space limitations, time constant curve is divided into 4 separate curves.

SHEATH DIAMETER .004" to .034"

SHEATH DIAMETER 1/32" to 3/8"

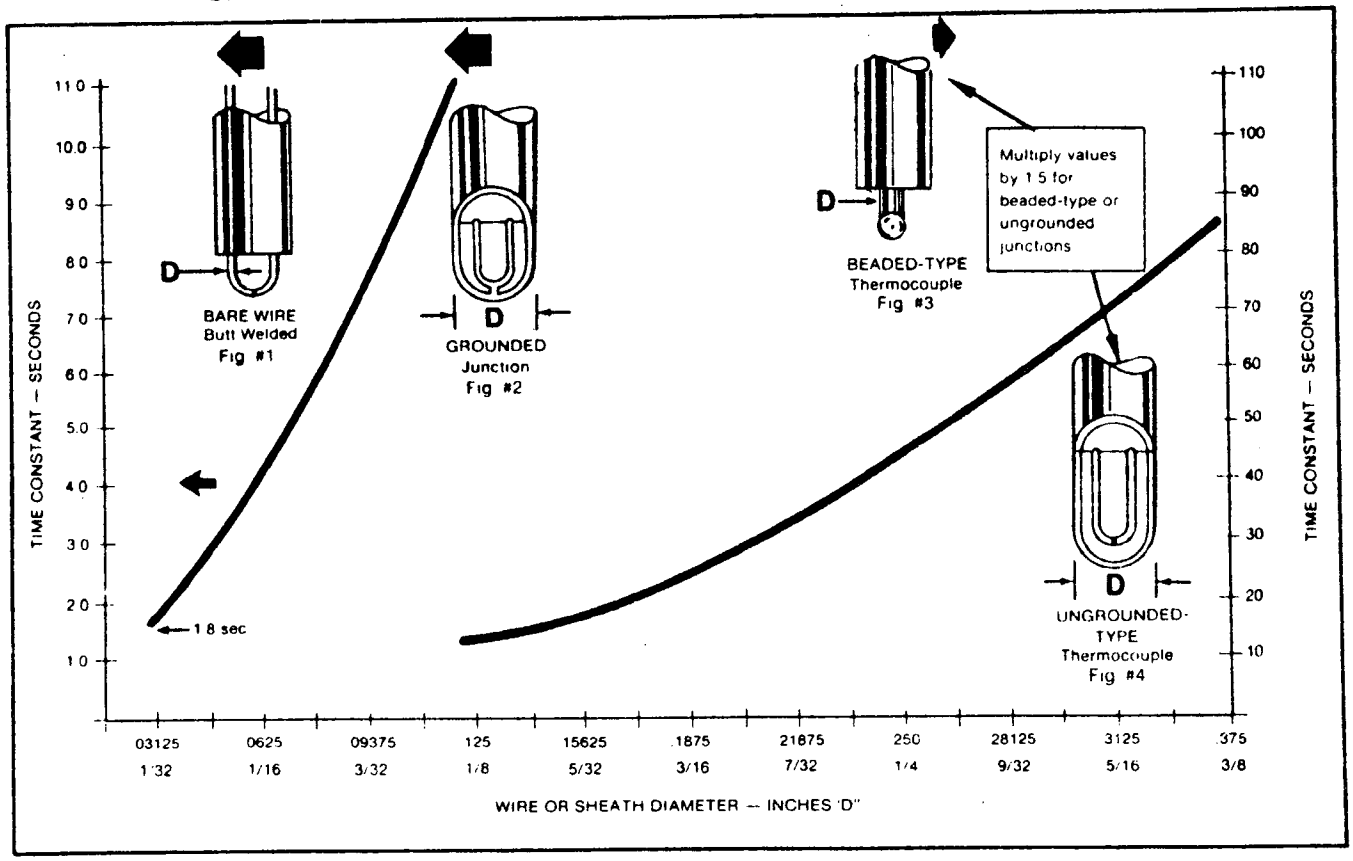

Note:

These comparisons apply to either bare "butt-welded" or "grounded" junction thermocouples. If the thermocouples are the "beaded-type" or "ungrounded" the time constant is longer. These times are only approximate and are for comparison purposes only. Multiply values from figures by 1.5 for functions shown in Fig #3 and Fig #4.

FIGURE 2

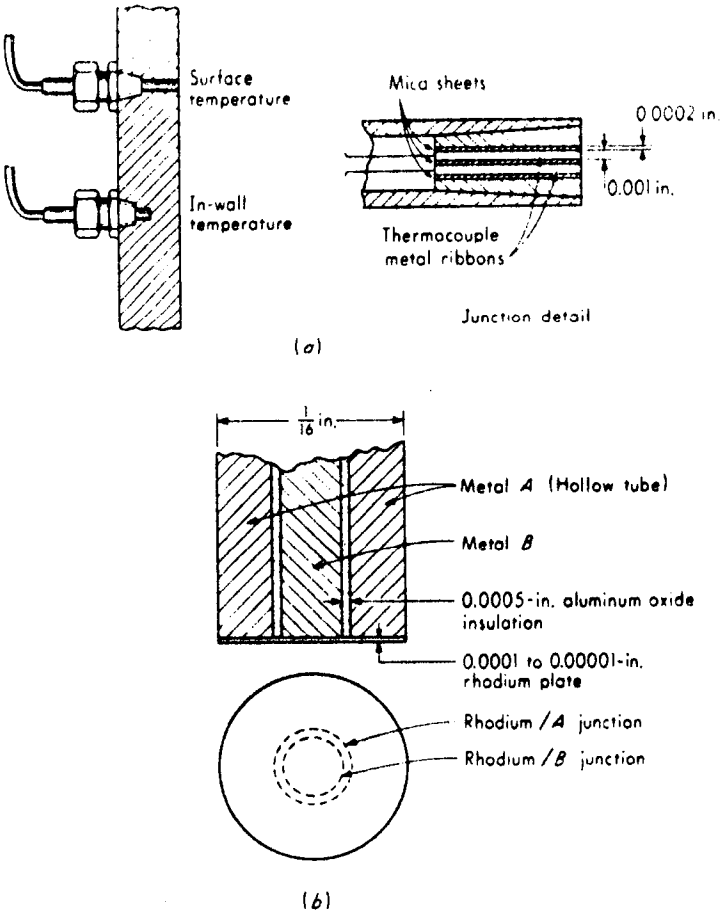

Fig. 3 ***High-speed thermocouples.***

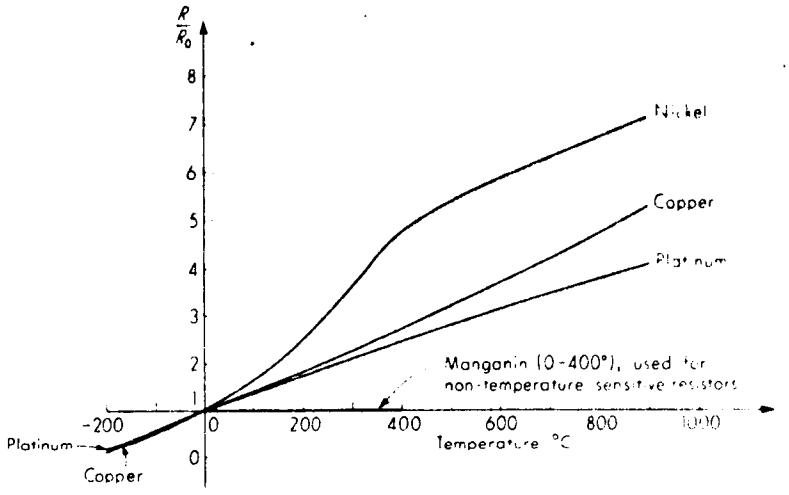

Fig. 4 *Resistance/temperature curves.*

and/or cooling jackets. The time constants in air for bare wire, grounded and ungrounded thermocouples are compared in Figure 2[2].

Common thermocouple wires range from about 0.51 to 2.54 mm in diameter, while inconel or stainless steel sheathed thermocouples range from 1.59 mm to 6.35 mm in diameter.

Fast response fine wire thermocouples (micro thermocouples) range in sizes readily available from 0.013 mm up, and thin foil thermocouples 0.005 mm thick are commercially available (response times $\leq$10 ms).

A rapid response thermocouple is also available as shown in Figure 3[3] where 0.025 mm thick flattened thermocouple wire is sandwiched between 0.005 mm thick mica sheets. Microscopic hot welded thermocouple junctions are formed by polishing the sensing tip. Such T/C's have time constants as small as 10 μs.

For most strong radiation fields, W-Re and Pt-Mo type thermocouples are recommended, since Pt-Rh type thermocouple has an output voltage drift due to the nuclear reactions.

17.2.2 Resistance Temperature Detectors or Sensors (RTD's)[4]

The variation of resistance R with temperature T for most metals may be represented by a resistance-temperature function as

$$R = R_o (1 + a_1 T + a_2 T^2 + \ldots + a_n T^n)$$

where R_o is the resistance at T_o (the triple point for water). Figure 4[3] shows the resistance curves for commonly used materials for RTD elements. It can be seen that platinum, nickel and copper require one, two and three constants "a" in the above equation to accurately represent their resistance change with temperature.

The sensing element is typically installed near the bottom of a stainless steel protective sheath as shown in Figure 5[5], and lead wires run to a resistance bridge. Figure 6 shows two, three and four-wire bridge networks. In the two wire RTD the only compensation is in the R_b leg of the bridge. R_b is set to the actual sensor (RTS) resistance plus an amount equivalent to the average resistance of the lead wires. The three wire RTD has almost total compensation of lead wire resistance changes by placing a third lead wire in series with R_b. The four wire RTD is fully corrected for lead wire resistance. Two equivalent lead lengths are in series with R_b to completely balance the bridge for any changes in lead wire resistance.

Three and four wire RTD's are used almost exclusively in CANDU site and lab applications.

Linear bridges which convert the resistance to a millivolt/degree output signal may be used so that a millivolt readout device such as a DVM or panel meter becomes a direct reading temperature indicator (see Figure 7[5]). Linear bridges and mating RTD's can be purchased with factory calibration.

Copyright M.I.E.S. 1982

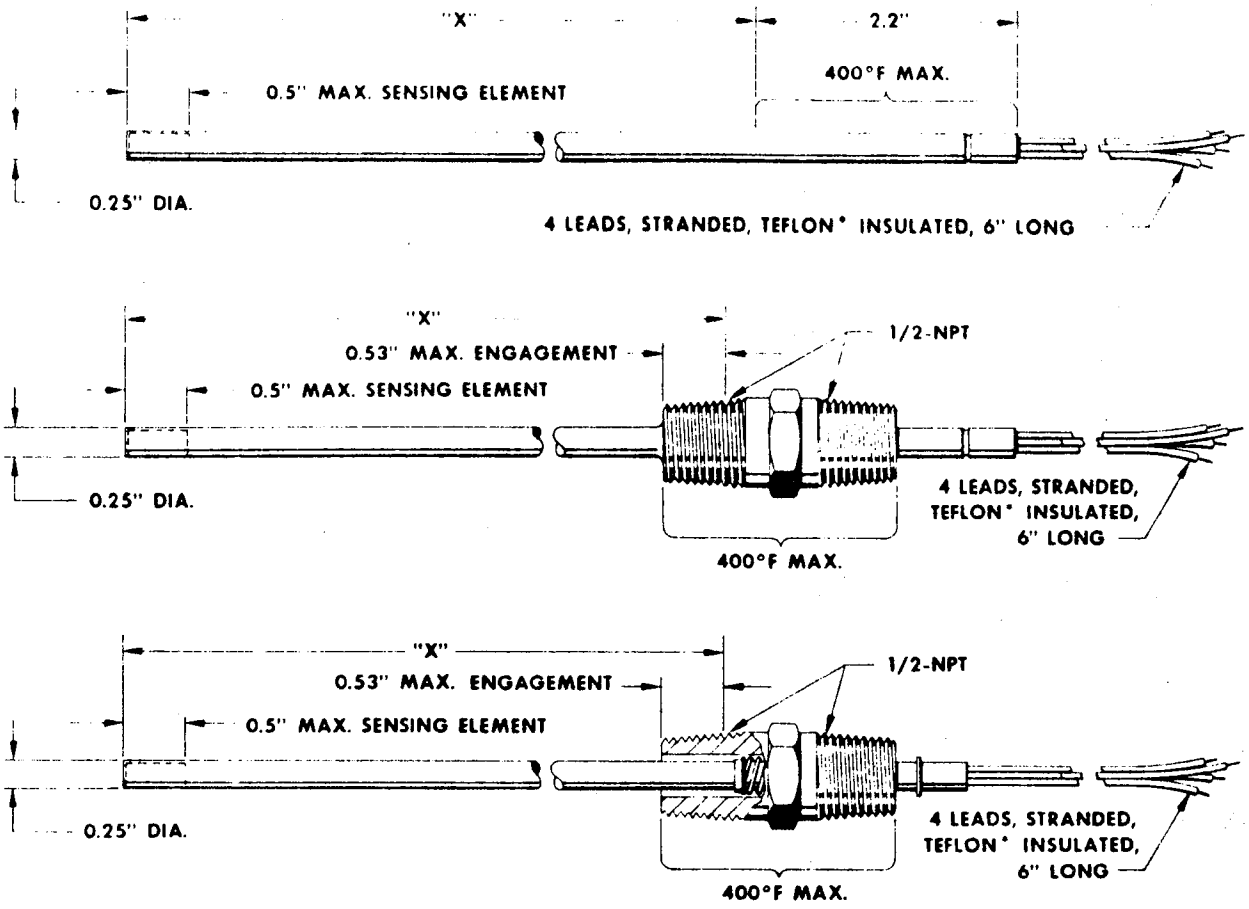

Figure 5: Stock Sensor Configurations

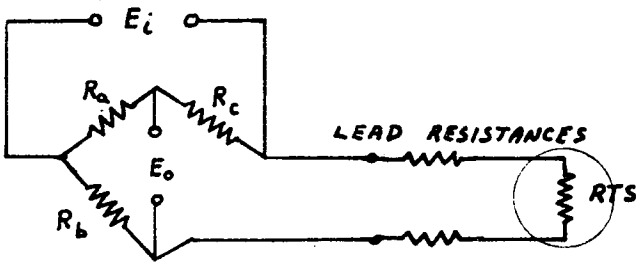

TWO-WIRE RTD AND BRIDGE

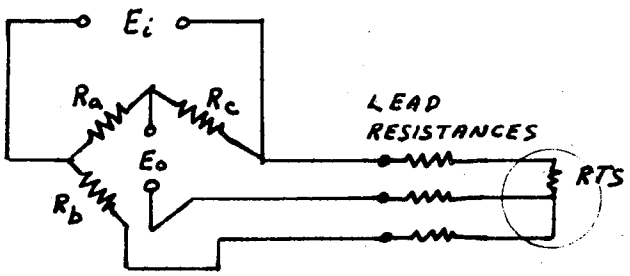

THREE-WIRE RTD AND BRIDGE

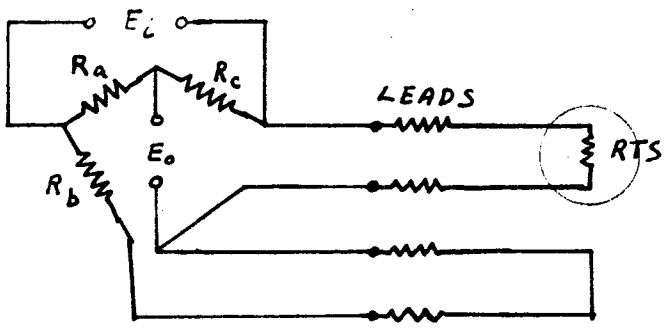

FOUR-WIRE RTD AND BRIDGE

FIGURE 6

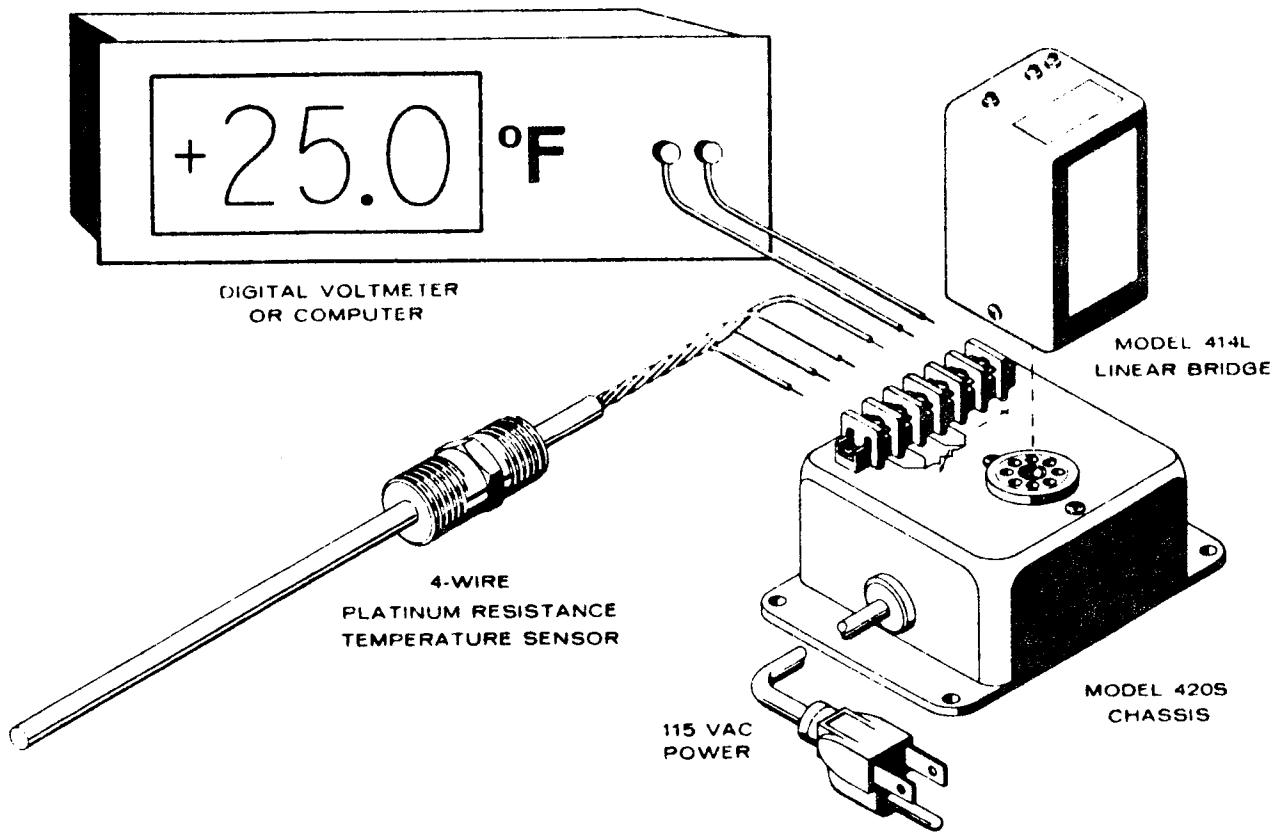

Figure 7: Typical Installation

MODEL 77B SENSOR ASSEMBLY WITH CONNECTION HEAD, EXTENSION AND THERMOWELL

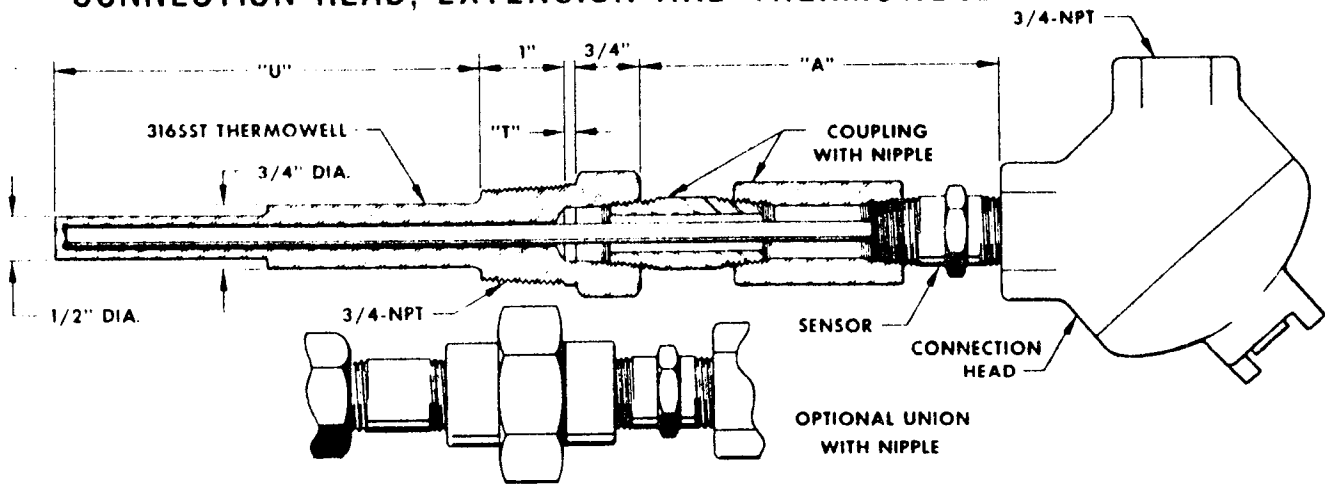

FIGURE 8

In large scale applications such as in CANDU reactors, the RTD's are factory calibrated and the constants for the resistance temperature equation determined and controlled for the lot of RTD's. These constants are then stored in site computers for digital temperature readouts, or printouts.

RTD's are used almost exclusively in CANDU nuclear power plants because of their ruggedness, accuracy and stability. Also if an RTD fails, it usually fails open circuited, so that the failure is obvious to the operators.

However, RTD's are much more expensive than thermocouples and are generally bulkier. RTD stems are typically 6.35 mm to 1.27 mm in diameter. Time constants are claimed[5] to be about 8 s for a bare RTD in water. However, for fluid temperature measurements stainless steel thermowells as shown in Figure 8[5] are often used. As a result the RTD response time (23-28 s in water[5]) is very slow compared to thermocouples, and RTD's are only used to record slow temperature transients, and steady-state temperatures.

In lab applications, smaller RTD's used without thermowells allow faster response, but for fast transients thermocouples should be employed.

17.3 PRESSURE

A basic list of devices to measure pressure includes:

dead-weight gauges
manometers
elastic (e.g. bourdon tube) transducers
strain gauge pressure transducers
piezoelectric pressure transducers
Force-balance (e.g. pneumatic) pressure transmitters
capacitance cell pressure transmitters

However, the two devices used most frequently in CANDU site and laboratory applications are the strain gauge (bonded, or semiconductor) and capacitance cell pressure transducers.

17.3.1 Strain Gauge Pressure Transducers

Strain gauge pressure transducers are generally used in applications where transient pressures are recorded. A typical differential pressure bonded strain gauge transducer is shown in Figure 9[6]. Bonded strain gauge transducers may be constructed with the gauges bonded directly to a diaphragm, or a beam, tube, or proving ring inside the pressure cell. Bridge networks are employed to compensate the strain gauges for temperature effects and to obtain an output voltage. Strain gauge pressure transducer frequency response is up to 100 kHz depending on the particular device.

Semiconductor pressure transducers make use of an integrated circuit sensor, typically consisting of a miniature silicon diaphragm on

Copyright M.I.E.S. 1982

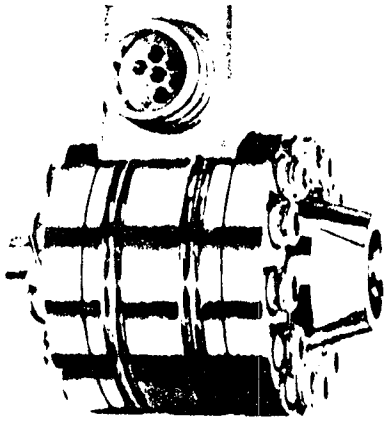

FIGURE 9
Bonded Strain Guage Pressure Transducer

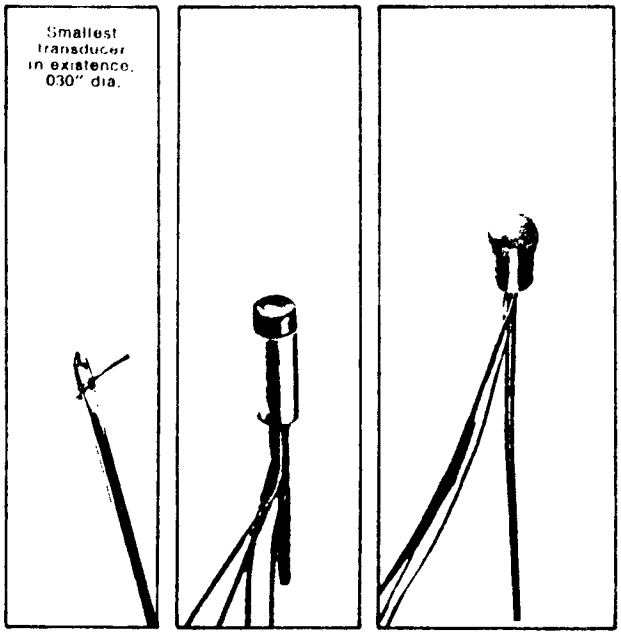

Ultra Miniature IS Pressure Transducers

FIGURE 10

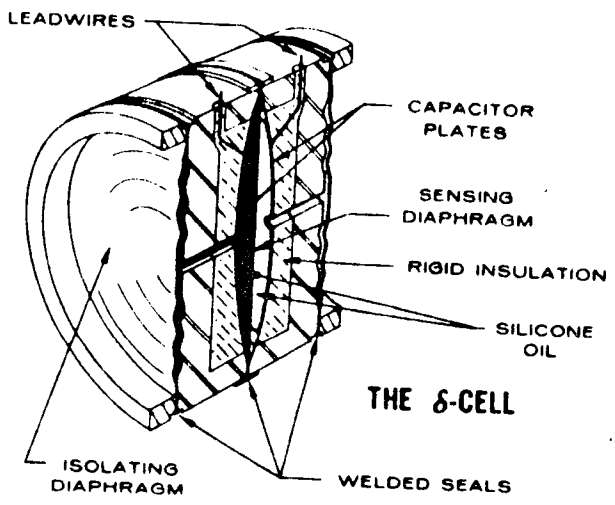

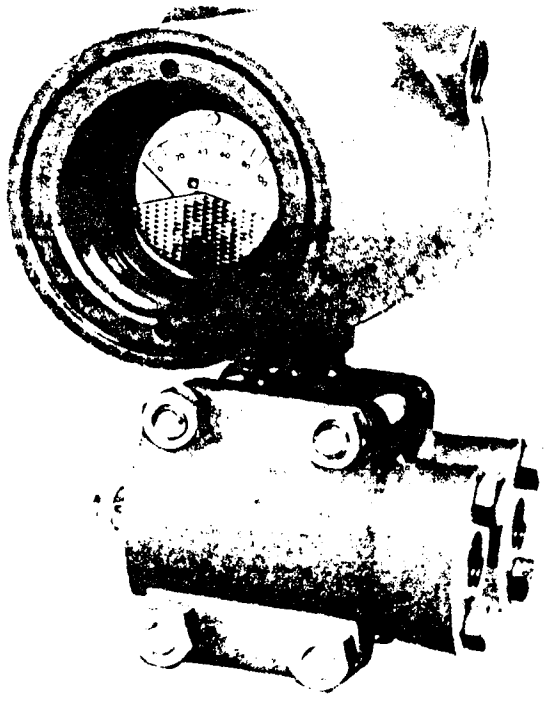

FIGURE 11 Capacitance-type pressure Transmitter

which a wheatstone bridge has been automatically bonded using diffusion techniques. The miniaturization achieved with semiconductor pressure transducers allows extremely small transducer sizes, as shown in Figure 10[7], and extremely high frequency response (up to 500 kHz).

17.3.2 Capacitance Cell Pressure Transmitters

A capacitance-type differential pressure transmitter is shown in Figure 11[8]. Process pressure is transmitted through isolating diaphragms and a silicon oil insulator to a sensing diaphragm in the center of the cell. The sensing diaphragm deflects in response to the differential pressure across it. The position of the sensing diaphragm is detected by capacitor plates and the differential capacitance between these plates is converted electronically to an electric current output signal.

Capacitance-type absolute and differential pressure transducers are used exclusively on CANDU reactors, as they are accurate, reliable, stable devices. However they are not well-suited for measurement of rapid transients, as their maximum frequency response is about 100 Hz.

17.4 QUALITY MEASUREMENT

The quality x of a two-phase mixture is defined as the mass fraction of the vapour phase to the total mass of the fluid. That is

$$x \equiv \frac{m_g}{m_g + m_f} = \frac{m_g}{M}$$

In CANDU reactor applications, the proper determination of the steam quality is important, as it is a thermodynamic parameter.

A similar parameter is the void fraction or vapour volumetric fraction defined as

$$\alpha \equiv \frac{v_g}{v_f + v_g} = \frac{v_g}{V}$$

Neither of these parameters is presently measured directly in a CANDU power plant, but they may be measured directly in supporting laboratory experiments. Typically the void fraction is measured with a gamma densitometer or other device, and then the quality determined from a void fraction-quality relationship. Quality may also be determined in experiments through heat balance calculations.

Quality is presently determined in operating stations basically through heat balance calculations. However, quality may be determined in future reactor outlet feeders using quality meters (orifice plates and/or venturimeters).

Copyright M.I.E.S. 1982

17.4.1 Heat Balance Calculations

In a reactor channel, sufficient heat addition may cause boiling to occur. In this case a heat balance may be written as

$$W \Delta h = Q$$

where W = channel mass flow rate, Q = channel power. Hence,

$$\Delta h = h_e - h_i = Q/W$$

$$h_{fe} + x_e h_{fge} - h_{fi} - x_i h_{fgi} = Q/W$$

$$x_e = (\underbrace{h_{fi} + x_i h_{fgi}}_{\text{or } h_\ell} + Q/W - h_{fe})/h_{fge}$$

Another case where quality is often calculated is downstream of a steam-water mixer in laboratory test rigs. For superheated steam and subcooled water entering the mixer as shown in the sketch, the quality at the exit of the mixer is simply calculated by a heat balance.

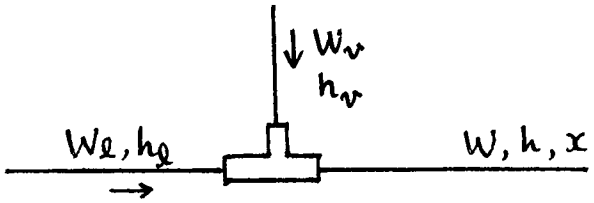

$$W_\ell h_\ell + W_v h_v = Wh$$

$$= W(h_f + x h_{fg})$$

$$\therefore \quad x = \frac{W_\ell h_\ell + W_v h_v - Wh_f}{W h_{fg}}$$

17.4.2 Orifice and Venturimeter Quality Metering

7.4.2.1 Single Phase Orifices and Venturimeters

For subsonic, single phase flows through an orifice or venturimeter, the mass flow rate is given[9] as

$$W\ (kg/s) = 1.11072 \frac{C \gamma d^2 F_a}{\sqrt{1-\beta^4}} \sqrt{\rho_1 \Delta P_N}$$

where C = discharge coefficient, (-)
Y = expansion factor, (-)
d = orifice, nozzle, venturi throat diameter, (m)
D = pipe diameter, (m)

Copyright M.I.E.S. 1982

F_a = thermal expansion factor, (-)
β = d/D = diameter ratio, (-)
ρ_1 = upstream density (kg/m^3)
$P_N = P_1 - P_2$ = differential pressure, (Pa)

an alternate form is

$$G\ (kg/sm^2) = \frac{C_1\ Y\ F_a}{\sqrt{1-\beta^4}}\ \sqrt{\rho_1\ \Delta P_N}$$

where C_1 also accounts for units.

17.4.2.2 Two-Phase Orifices

For two-phase flows, the following correlations for orifices are among many that have been proposed.[10]

$$G = \frac{C\ Y\ F_a}{\sqrt{1-\beta^4}}\ \left(\frac{\Delta P_N}{x^{1.5}\ (v_g - v_f) + v_f}\right)^{1/2}\ ,\ \text{James (1966)}$$

$$G = \frac{K'_g\ Y_g\ F_a\ \sqrt{\rho_g\ \Delta P_N}}{x + 1.26(1-x)\ \frac{K_g\ Y_g}{K_f}\sqrt{\frac{\rho_g}{\rho_f}}}\ ,\ \text{Murdock (1962)}$$

$$G = \frac{C_f}{\sqrt{1-\beta^4}}\ \phi^x\ \left[\frac{1-\alpha}{1-x}\right]\ \sqrt{\rho_f\ \Delta P_N}\ ,\ \text{Marriott (1970)}$$

where ϕ is a parameter

$$G = \frac{C_g\ Y_g\ F_a}{x\ \sqrt{1-\beta^4}}\ (BF)\ \sqrt{\rho_g\ \Delta P_N}\ ,\ \text{Smith \& Leang (1975)}$$

where $BF = 0.637 + 0.4211\ x - \frac{0.00183}{x^2}$

The use of James correlation for steam water flow (accuracy within ±8.1%), and the use of Murdock's correlation for two-component gas liquid flow (±7.4%) has been recommended.[10]

More recently, a correlation by Lin[11] (1981) is given as

Copyright M.I.E.S. 1982

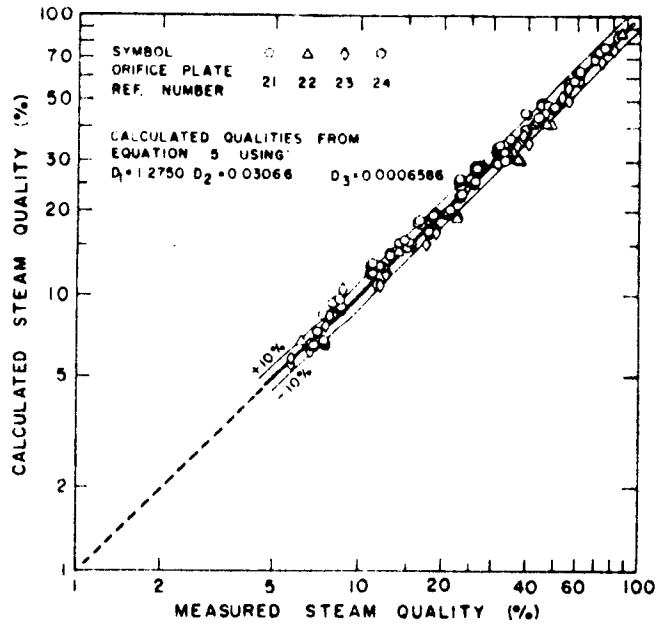

Fig. 12 Variation of measured with calculated steam qualities—orifice plates

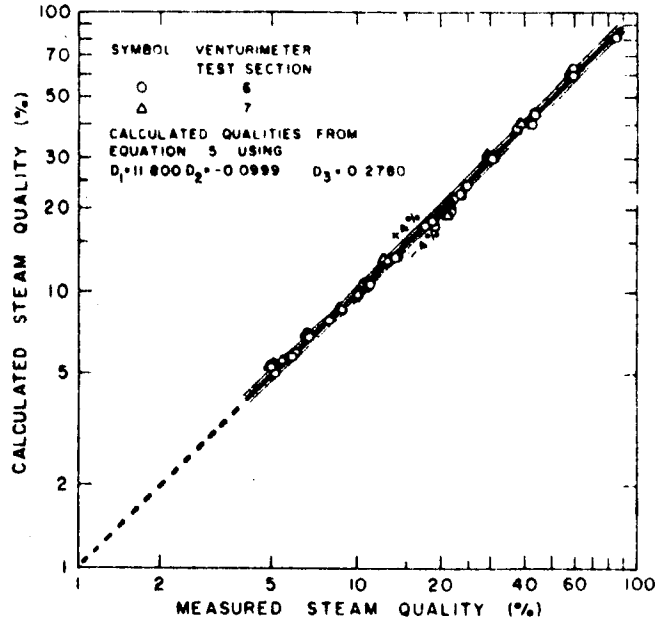

Fig. 13 Variation of measured with calculated steam qualities—venturimeters

DATA

Murdock (1962)

Chisholm & Watson (1966)

Bizon (1965)

James (1966)

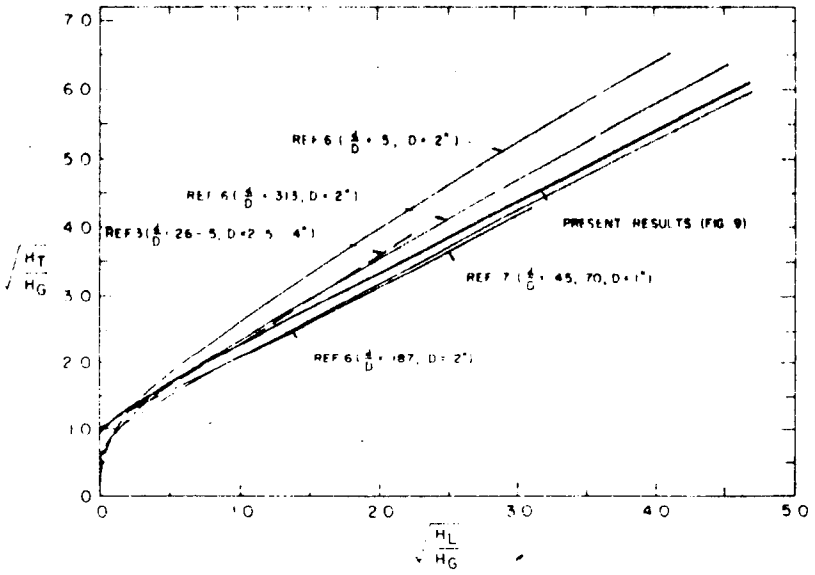

Fig. 14 Comparison of present results with other data

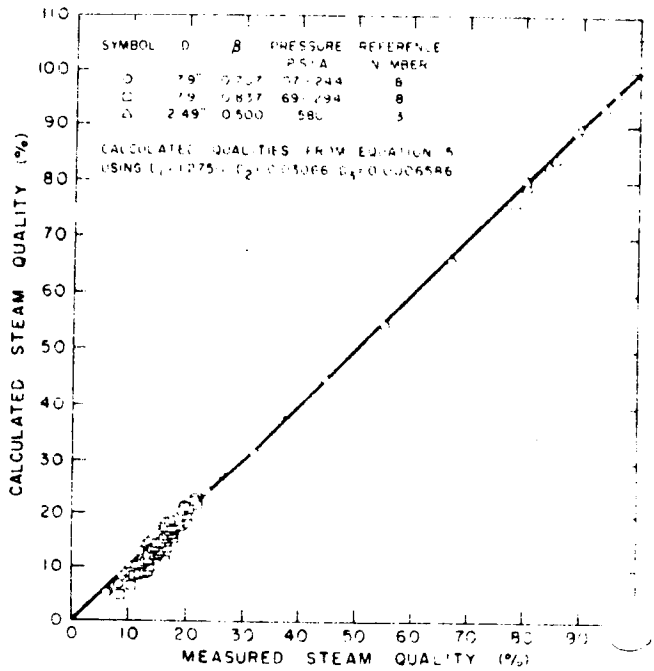

Fig. 15 Comparison of data from references [3, 8] with values calculated from present correlation

$$G = \frac{C F_a \sqrt{2 \rho_\ell \Delta P}}{\sqrt{1-\beta^4}\left[(1-x)\theta + \frac{x\sqrt{\rho_\ell}}{\sqrt{\rho_g}}\right]}$$

and an RMS error within 10% found.

17.4.2.3 Two-Phase Orifices and Venturimeters

A correlation developed by Collins and Gacesa[12] (1970) is given as

$$\Delta P_N \text{ (psia)} = 0.0361\, W^2\, v_g\, (10^{-8}) \left[\frac{\frac{D_1}{Y} - R}{2D_3 K_1 d^2}\right]^2 \left\{-D_2 + \left[D_2^2 - 4D_3\left(-x - \frac{R}{(\frac{D_1}{Y} - R)}\right)\right]^{1/2}\right\}^2$$

where

$$R \equiv \sqrt{\frac{\rho_g}{\rho_f}}, \quad K_1 \equiv \frac{C F_a}{\sqrt{1-\beta^4}}$$

For orifices $D_1 = 1.2750$
$D_2 = 0.03066$
$D_3 = 0.0006586$

and for venturimeters $D_1 = 11.800$
$D_2 = -0.0999$
$D_3 = 0.278$

Figures 12 and 13[12] show that the accuracy of Collins and Gacesa's method of predicting steam quality by measuring ΔP is within 10% for their orifice data, and 4% for venturimeter data. Figures 14 and 15 show good agreement with James', Murdock's, Chisholm's and Bizon's data.

17.5 FLOW RATE AND VELOCITY MEASUREMENTS

Flow rate and velocity measurement can be categorized as follows:

(1) Optical velocimeter
(2) Ultrasonic velocimeter
(3) MHD flow meter

Copyright M.I.E.S. 1982

(4) Voltex type flow meter
(5) Turbine flow meter
(6) Drag disc
(7) Venturimeter/orifice plate
(8) Pitot tubes
(9) Hot wire probes
(10) Coriolis force type flow meter
(11) Tracer technique.

Except for optical velocimeters the other measurement techniques are commonly used in nuclear power plants and industries. Typical ranges of tube size as a function of cost for various flow- and velocimeters is shown in Figure 16. The techniques are categorized as non-interfering or interfering, flow rate or velocity measurements. The applicability for two-phase flow is shown in Table 2.

17.5.1 Turbine Flow Meter

A typical turbine flow meter is shown in Figure 17. It consists of a five-blade rotor supported by radial ball bearings. The speed of rotation is related to the volumetric flow and is sensed by a magnetic pickup mounted on the flow tube. An application of turbine flow meter under the two phase flow conditions was studied by Aya (1975)[13], Rouharin (1974)[14] and Heidrick et al. (1978)[15]. Results show that the mass flow rate, m can be obtained reasonably well under two-phase conditions by the formula

$$\dot{m} = A\ V_T\ \{\varepsilon_g\ \rho_g + (1 - \varepsilon_g)\ \rho_\ell\}$$

in the range from 0.1 to 4 ($\mu g/m^2 \cdot s$), where the average blade velocity in the direction of flow, V_T, is

$$V_\tau = \frac{1}{R} \int_0^R \frac{r\omega}{\tan\phi}\, dr$$

if simple turbine models can be derived by using Figure 17 (Aya 1975)[13].

7.5.2 Drag Disc

Basic idea of drag disc is shown schematically in Figure 18. The effect of flow velocity on the drag of disc plate is converted to the displacement angle θ as shown in Figure 18. The mass flux can be obtained by

$$\dot{m} = A \sqrt{\rho(\rho u^2)} = A \sqrt{\frac{2\rho\ K\theta}{A_d\ LC_D}}$$

for single phase flow, and the liquid phase velocity can be obtained from

Copyright M.I.E.S. 1982

TABLE 2

Method	Interfering	Flow Rate	Applicable to two phase flow
Optical velocimeter	No	No	Yes
Ultrasonic velocimeter	No	Yes/No	Yes
MHD flow meter	No	Yes	Yes
Voltex type flow meter	Yes	Yes	No
Turbine flow meter	Yes	Yes	Yes
Drag disc	Yes	Yes	Yes
Venturi/orifice meter	Yes	Yes	Yes
Pitot tubes	Yes	No	No
Hot wire probes	Yes	No	No
Coriolis force type flow meter	Yes	Yes	No
Tracer technique	No	Yes	Yes

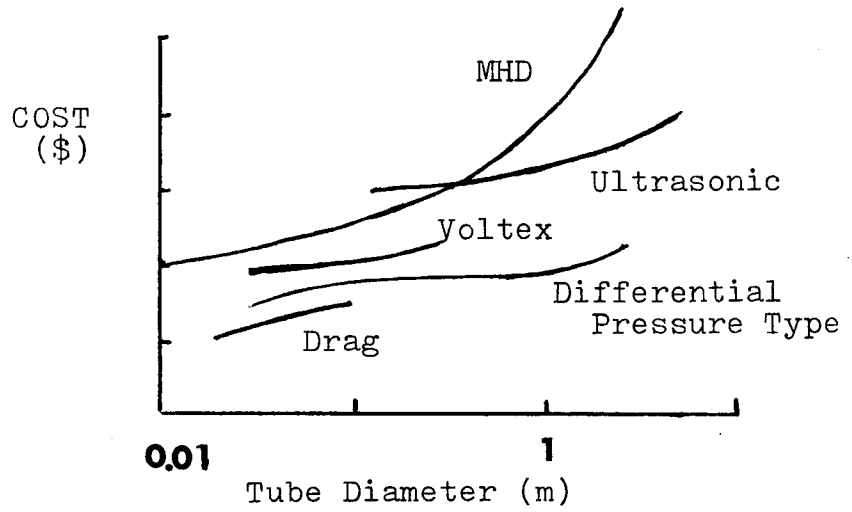

Fig. 16: Cost of flowmeters vs. tube diameters.

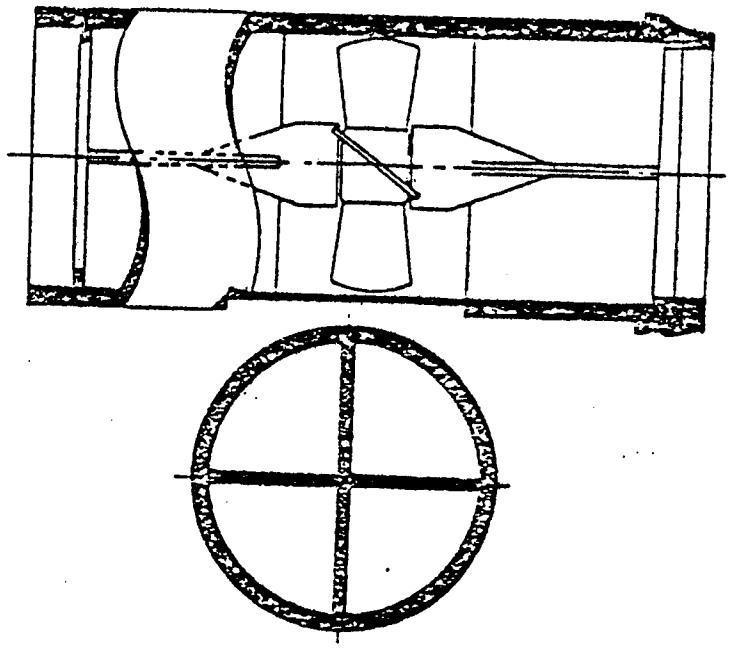

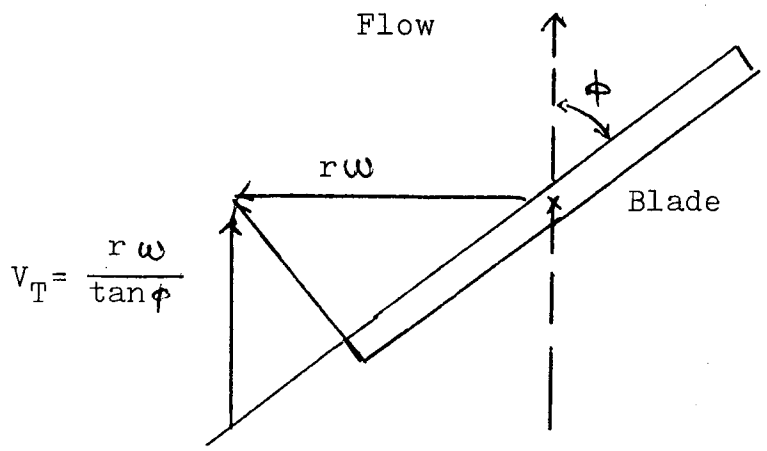

Fig. 17: A schematic diagram of a turbine flow meter, and turbine blade element with velocity vectors.

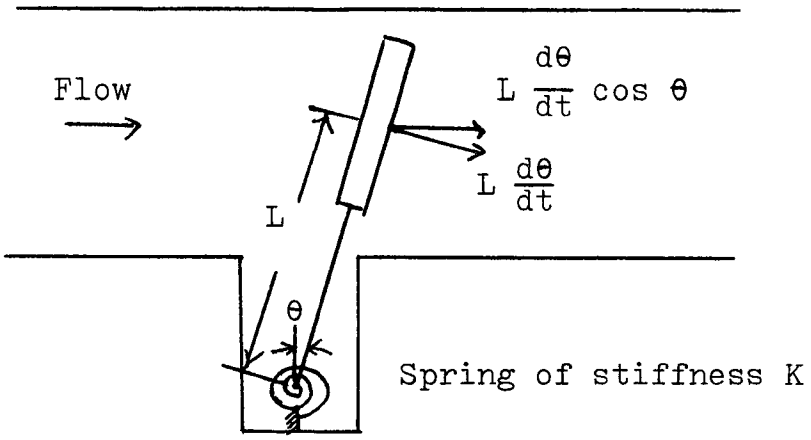

Fig. 18: Schematic diagram of a drag disc.

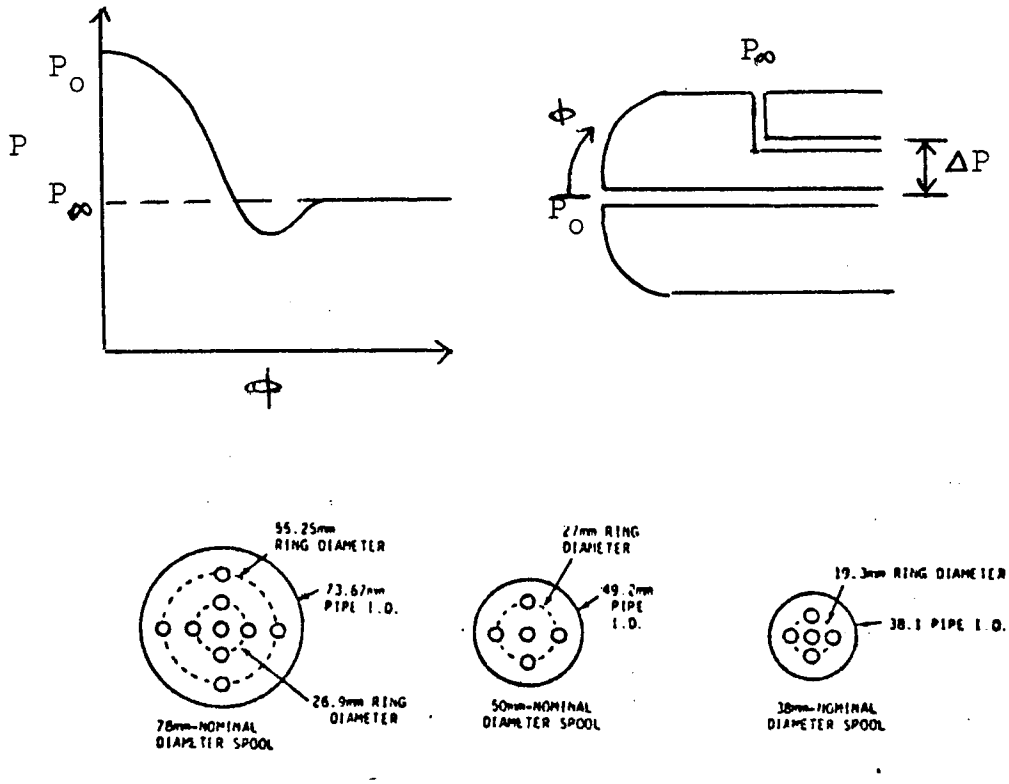

Fig. 19: Principle of pitot tube operation and pitot tube rake configurations for momentum flux measurements (Heidrick et al., 1978).

$$u_\ell = \sqrt{\frac{2\,K\theta}{A_d\,L\,C_D\,C_d\,[\varepsilon_g\,\rho_g\,S^2 + (1-\varepsilon)\,\rho_\ell]}}$$

under two phase flow (Sheppard et al., 1976), where C_D is a drag coefficient, A_d is the disc area, C_d is a coefficient that incorporates the effects due to non-homogeneity in the distribution of gas on liquid phase, and $C_{d\ell} = C_{dg} = C_d$ is assumed in the above equation.

17.5.3 Pitot Tube

From the Bernoulli equation, Re $\to \infty$, the total pressure can be expressed by

$$p + 1/2\ \rho u^2 = p_o \equiv \text{total pressure}$$

Therefore, if we used blunt object as shown in Figure 19, we obtain undisturbed velocity as follows

$$U_\infty = \sqrt{2\ (p_o - p_\infty)/\rho}$$

where velocity can be determined from the pressure difference as shown in Figure 19.

In the two-phase flow, an array of Pitot tubes can also be used to determine the cross-section averaged momentum flux as shown in Figure 19. Several different methods of interpreting the Pitot tube measurements were tried. In general, the simplest method was the most successful; the cross-section average mass flow rate was assumed to have the form (Heidrick et al. 1978)[15]

$$\dot{m} = A\ C_p \sqrt{\rho\ \overline{\Delta p}}$$

where C_p is a pressure coefficient obtained from experiments with single-phase liquid flow and $\overline{\Delta p}$ is the dynamic pressure taken over all Pitot tubes. From a comparison of actual measured mass fluxes, determined using the above equation and ρ calculated assuming homogeneous flow, for a range of steady steam-water flows at 0.1 to 4 Mg/m^2s, it can be seen that this method of interpreting the Pitot tube measurements gives results which agree well with the experiment (Heidrick et al. 1978).

17.5.4 Venturi Meters and Orifice Plates (see also 17.4)

Venturi meter shown schematically in Figure 20a. From the Bernoulli equation, the flow rate can be obtained by

$$Q = u_2\,A_2 = \sqrt{\frac{A_1^2\,A_2^2}{A_1^2 - A_2^2}\ 2g\ \left(\frac{p_1 - p_2}{\rho} + h_1 - h_2\right)}\quad m^3/sec)$$

Copyright M.I.E.S. 1982

or $Q = C\sqrt{(p_1 - p_2)/\rho}$ where $C = B_1 \dfrac{A_1 A_2 \sqrt{2g}}{\sqrt{A_1^2 - A_2^2}}$ (horizontal)

where A is the cross sectional area, h is the elevation head, and B_1 is the sectional area coefficient from calibrations.

Typical orifice plates are shown in Figure 20b. Again from the Bernoulli equation, the flow rate of liquid can be obtained from

$$\dot{M} = KA_2 \sqrt{2\rho_\ell (p_1 - p_2)}$$

and

$$K = C/[1 - (A_2/A)^4]^{1/2}$$

where C is the discharge parameter obtained from experimental calibrations. For a compressible gas, we obtain a further coefficient y from the experimental calibrations, such that

$$\dot{M} = y\ K\ A_2 \sqrt{2\rho_g (p_1 - p_2)}$$

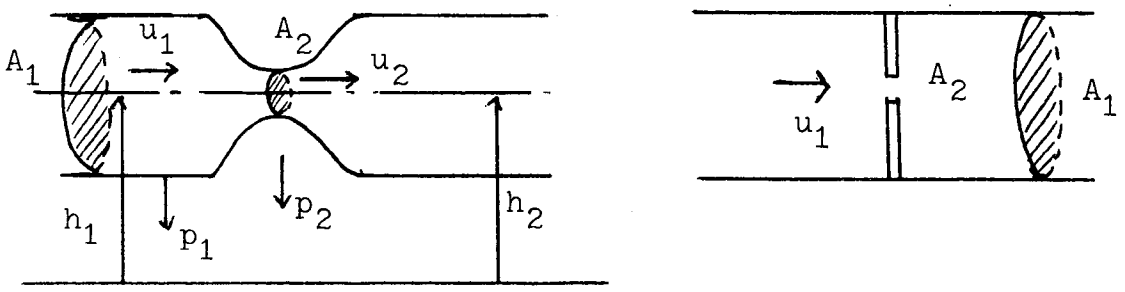

Fig. 20: Venturimeters (a) and Orifice plates (b).

17.5.5 Tracer Techniques

Tracer technique is shown in Figure 21. The pulsed injected tracer gas or solid particles will be transported and diffused by fluid flows, and detected at downstream locations. From the distance between injection and detection point $\Delta\ell$ and time lag Δt, we obtain

$$U = \Delta\ell/\Delta t \ [m/sec]$$

However, due to the diffusion effect these entrained particles are not a simple function of $\Delta\ell$ and Δt. The formula to control this phenomena is

Copyright M.I.E.S. 1982

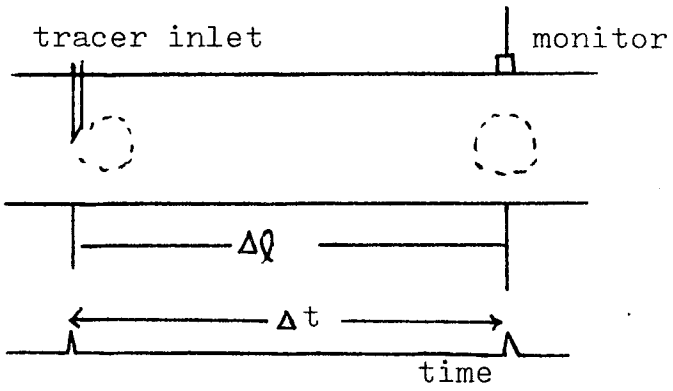

Fig. 21: Tracer technique.

$$\frac{\partial N}{\partial t} + \nabla \cdot (\underline{U} + \underline{U}_g) N - \nabla \cdot (D \nabla N) = 0$$

and this solution must be obtained in each individual case. In metallic pipes, gamma-emitting tracer or neutron-activated tracers are generally used and listed in Table 3.

17.5.6 Ultrasonic Flow Meters

Ultrasonic flow meters measure the velocity of fluid flow through the interaction of an interrogating wave and the fluid flow or by sensing vibrations generated by the flow. Eight different types of ultrasonic flow measurement principles are shown in Figure 22, and as follows (Lynnworth 1979)[17].

1. Contrapropagating transmission methods (or transit time method).
2. Doppler shift method.
3. Beam drift method.
4. Time of flight method (or cross correlation method).
5. Vortex shedding method.
6. Liquid level method.
7. Acoustic emission method.
8. Hot wire waveguide.

In this section, due to the page limitation, the most widely used Doppler shift and the contrapropagating transmission method are presented. However, it is worth knowing that the cross correlation method is presently very promising.

(i) Contrapropagating Transmission Method

Typical flow cell and transducer designs used in the contrapropagating transmission method is shown in Figure 23. This method is based on the principle that the sound propagation velocity in fluid flow, W_f, is

$$W_f = C + V \quad \text{(downstream)}$$

or

$$= C - V \quad \text{(upstream)}$$

Copyright M.I.E.S. 1982

Table 3

Gamma-Emitting Gas Tracers

Isotope	$T_{\frac{1}{2}}$	Eγ(MEV)	Form
Ar-41	110 min	1.37	gas
As-76	26.5 hr	0.55-2.02	ASH_3
Br-82	36 hr	0.55-1.32	CH_3Br
Xe-133	5.27d	0.03,0.08	gas

Gamma-Emitting Traces for Liquid

Isotope	$T_{\frac{1}{2}}$	Eγ(MEV)
Mn-56	2.6 hr	0.85-2.11
Br-82	36 hr	0.55-1.32
I-131	8.1 d	0.364-.637
Au-198	2.7 d	0.412
Na-24	15 hr	1.37, 2.75
Cu-64	12.8 hr	0.51

Thermal Neutron-Activated Tracers

Element	$T_{\frac{1}{2}}$	Eγ(MEV)	σ (barns)
Eu	9.2 hr	0.84	670
Dy	2.3 hr	0.71	790
In	54 min	1.27, 2.09	148
Au	2.7 d	0.412	98

Elements Activated by 14.7 MeV Neutrons

Reaction	$T_{\frac{1}{2}}$	Eγ(MEV)	σ(mbarns)
$Na^{23}(n,\alpha)F^{20}$	11s	1.63	170
$O^{16}(n,\alpha)N^{16}$	7.14s	6.13, 7.11	33
$Mg^{24}(n,\alpha)Na^{24}$	15 hr	1.38, 2.75	180
$A^{27}(n,\alpha)Na^{24}$	15 hr	1.38, 2.75	110
$Si^{28}(n,\alpha)A^{28}$	2.3 min	1.78	200
$Ba^{138}(n,2\eta)Ba^{137}$	2.6 min	0.662	1250

Fig. 22

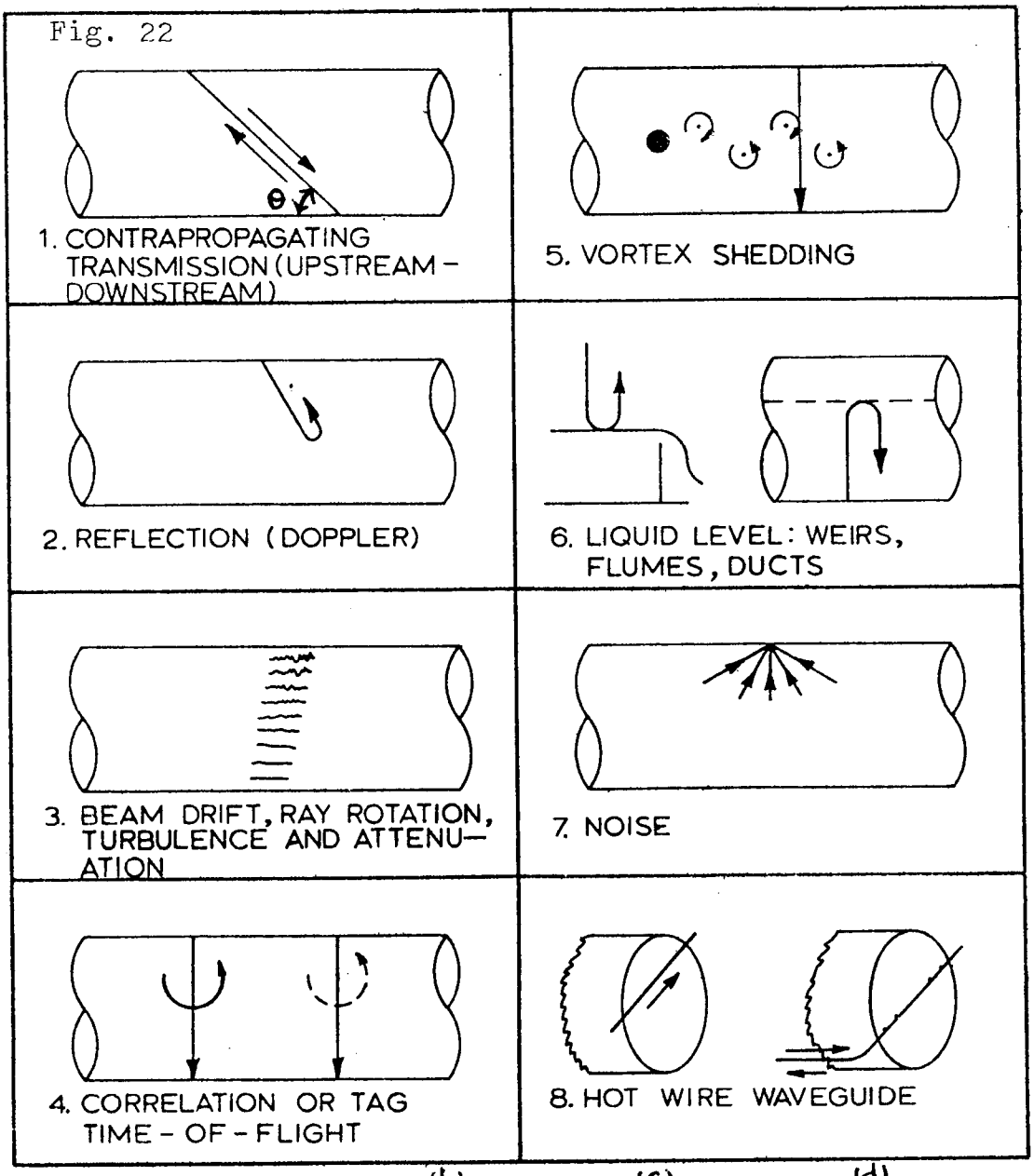
θ
1. CONTRAPROPAGATING TRANSMISSION (UPSTREAM – DOWNSTREAM)
5. VORTEX SHEDDING
2. REFLECTION (DOPPLER)
6. LIQUID LEVEL: WEIRS, FLUMES, DUCTS
3. BEAM DRIFT, RAY ROTATION, TURBULENCE AND ATTENU– ATION
7. NOISE
4. CORRELATION OR TAG TIME – OF – FLIGHT
8. HOT WIRE WAVEGUIDE

Fig. 23

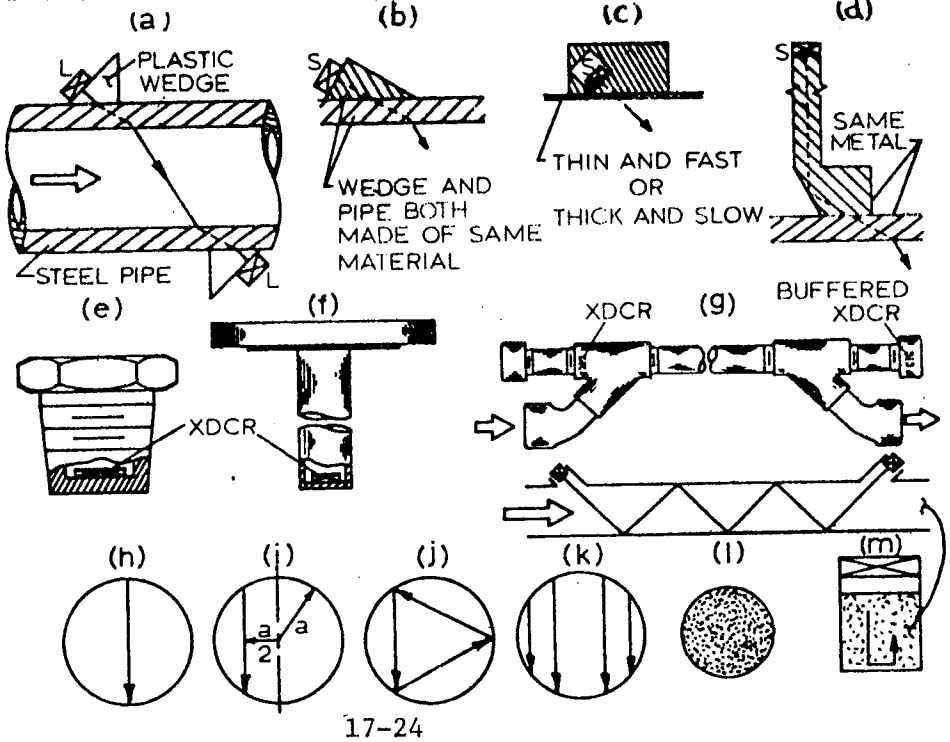
(a)
(b)
(c)
(d)
PLASTIC WEDGE
STEEL PIPE
WEDGE AND PIPE BOTH MADE OF SAME MATERIAL
THIN AND FAST OR THICK AND SLOW
SAME METAL
(e)
(f)
XDCR
(g)
XDCR
BUFFERED XDCR
(h)
(i)
(j)
(k)
(l)
(m)

where C is the sound velocity of fluid without flow and V is the fluid velocity. If we have two transducers a distance L apart, differences between downstream and upstream transmission times becomes

$$\Delta t = 2L\ V/C^2$$

Therefore, we can obtain velocity of fluid from the measurement of Δt. However, due to the temperature dependence of the sound velocity (eg. 0.3% per $1^{\circ}C$ for water), the method currently being used evaluates the inverse times,

$$\Delta f = 2V\cos\theta/L$$

where Δf is the difference between inverse sound transmission times for downstream and upstream directions (see Fig. 22).

This type of ultrasonic flow meter is commonly available with applications mainly in liquids, for temperatures up to $300^{\circ}C$, 3000 psig with 0 (1%) accuracy from 0.03 to 10 m/s or higher flow velocity ranges. The fastest response time in this method is approximately 10 msec.

(ii) Doppler Shift Method

Typical transducer arrangements applied to duct flow based on the Doppler shift method are shown in Figure 24. This method has a relative advantage as applied in two-phase flow systems. Doppler shift methods are based on the principle that the frequency of ultrasonic waves reflected from scatterers within the moving medium is shifted in proportion to the velocity of the scatterers. The differences between sending and receiving signal frequencies (f_s and f_r, respectively) are

$$f_d = |f_r - f_s| = 2\ Vf_s/C.$$

Again, main sources of error arise from the variable sound velocity in the above equation. A typical ultrasonic Doppler shift flow diagnostic system is shown in Figure 25.

17.5.7 Optical Velocimeters

Optical velocimeters are particularly important because they do not perturb the flow medium. They are also capable of very accurate measurements over an extremely wide velocity range, i.e., even in both laminar and turbulent flow, together with excellent resolution. One disadvantage is that small particles are required in the fluid to allow scattering of light in the flow region of interest; however, usually sufficient natural particles, even after fluid treatment, do exist in the system, and additional seeding is usually unnecessary.

Optical velocimeters can be classified as

(1) Coherent mode velocimeter: ex Laser Doppler DLDV method, etc.

(2) Incoherent mode velocimeter: ex White light fringe image method (WVIF) etc.

Copyright M.I.E.S. 1982

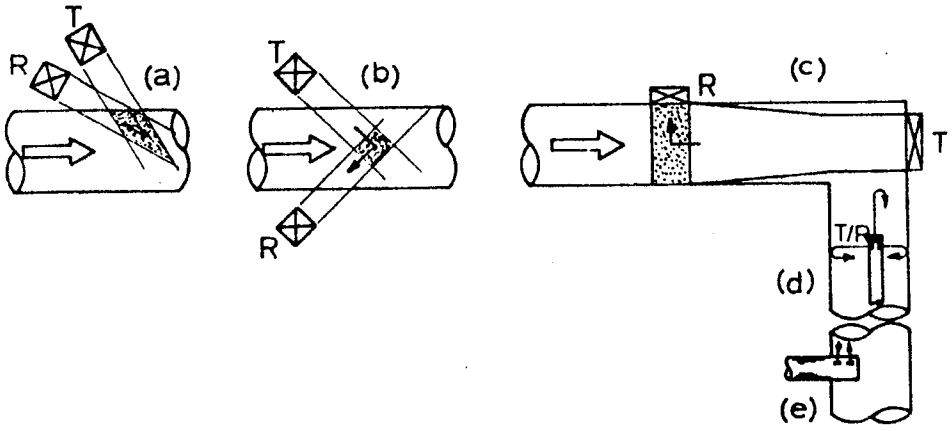

Fig. 24: Transducer arrangements applied to duct flow based on the Doppler effect.

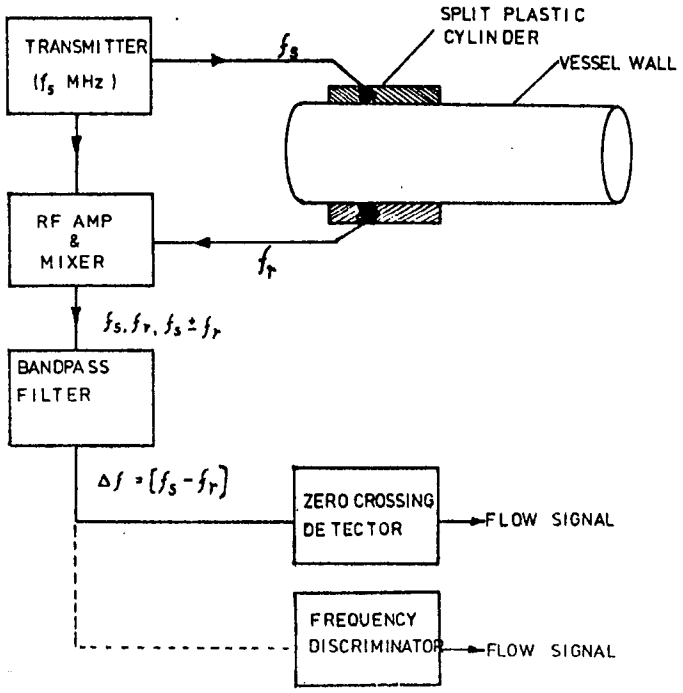

Fig. 25: Block diagram of a non-directional Doppler shift flow transduction system.

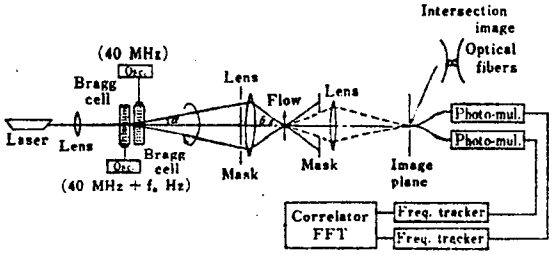

Fig. 27: The laser Doppler velocimeter for reduction of ambiguity noise.

Table 4: Optical and Geometrical Parameters for the DLDV and the WFIV Employed in the Laminar Flow Measurements.

Parameter	DLDV	WFIV
Light source	He-Ne laser	Tungsten filament
Wavelength	6328Å	White light
Wavefront	Coherent	Incoherent
Fringe spacing	1.6 μm	6.4 μm
Number of fringes	23 ± 2	40 ± 2
Fringe visibility	0.93	0.55
Longitudinal extent of the probe volume	171 μm	130 μm
Lateral extent of the probe volume*	34.3 μm	252 μm
Probe Volume	1×10^{-7} cm^3	3.3×10^{-6} cm^3
Detection angle	0^o	30^o
Flow seeding	25 wppm	50 wppm
Number of particles in the probe volume	19	1.6

* Both have circular cross-section.

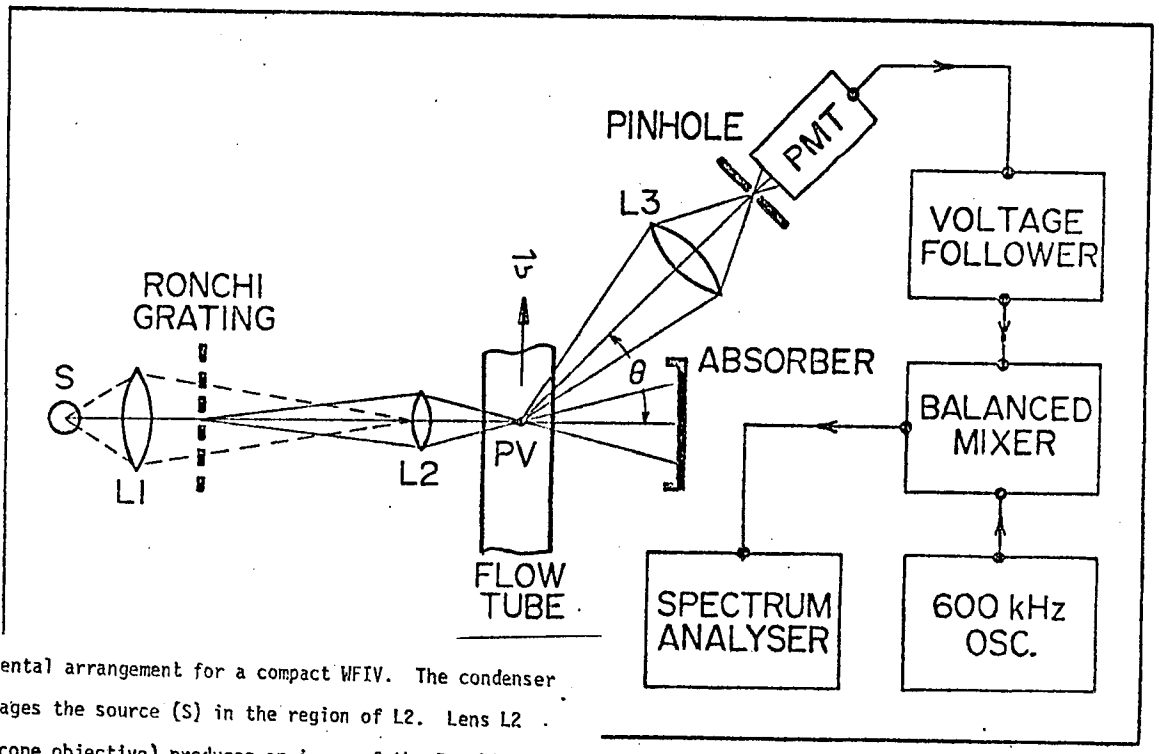

Fig. 26

Experimental arrangement for a compact WFIV. The condenser (L1) images the source (S) in the region of L2. Lens L2 (microscope objective) produces an image of the Ronchi grating in the probe volume (PV). A standard "35 mm" camera lens (f = 50 mm) is employed for the receiver lens (L3).

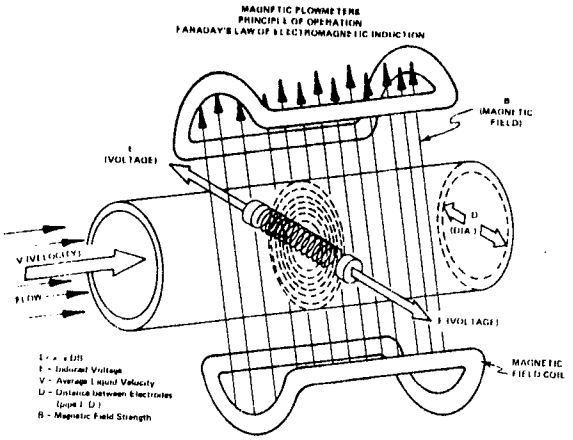

Fig. 28 Principle of operation of MHD flow meters.

The typical laser Doppler velocimeter used in turbulent flow is shown in Figure 26 (Nakatani et al. 1978). In the turbulent flow, ambiguity noise must be removed or reduced as shown in the block diagram in Figure 26. A typical White light fringe image velocimeter is shown in Figure 27 and specifications compared in Table 4 (Chan and Ballik, 1979). Table 4 shows that White light fringe image method has a potential advantage in long-term stability over the coherent velocimeter; however, it may need much larger particles for scattering.

17.5.8 MHD Flowmeter

Principle of MHD flow meter is shown in Figure 28. If fluid has a little conductivity, the electric field generated from the fluid average velocity and magnetic field becomes

$$v = BL\bar{u} \text{ [volt]}$$

from Fleming's right hand rule, where v is the voltage, $\underline{B}$ is the magnetic flux density, L is the characteristic length and $\bar{u}$ is the average velocity.

17.6 LIQUID LEVEL METERS

Water inventory of PHT system is usually monitored in a pressurizer. Typical sensing methods are listed in Table IV for various application ranges (Belsterling 1981). Principles of most important methods are shown in Figure 29.

17.7 VOID FRACTION AND OTHER ADVANCED DIAGNOSTIC TECHNIQUES

17.7.1 Void Fraction and Liquid Film Thickness

Measurements of various flow parameters are essential to two-phase monitoring systems or process control. Of these parameters, void fraction and liquid film thickness are the most difficult to measure among others, and are still in the research stage. Most commonly used techniques for void fraction measurement are

(A) Attentuation Methods

1. α, β, γ, X-rays and neutron beams.
2. Ultrasonic beams.
3. Optical and microwave beams.

(B) Scattering Methods

1. Fast neutron beams.
2. Ultrasonic beams.
3. Optical laser beams.

(C) Electrical Methods

1. Conductance probes.

Copyright M.I.E.S. 1982

Table IV

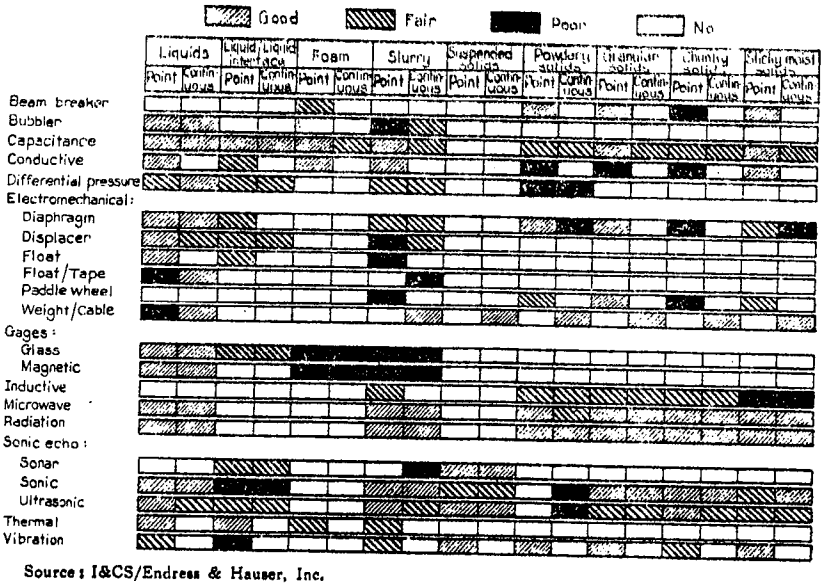

Source: I&CS/Endress & Hauser, Inc.

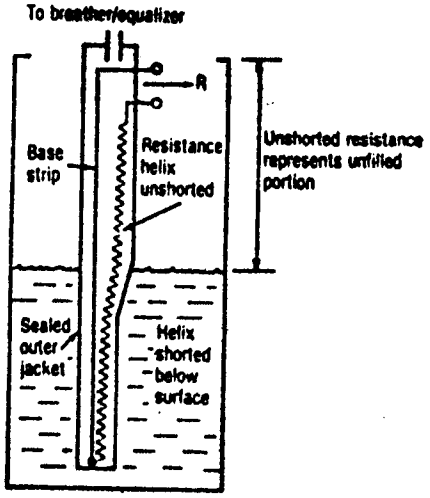

Resistance tape is shorted out as the level rises. Unshorted resistance measures distance from the top of the liquid to the beginning of the tape. Source: Metritape, Inc.

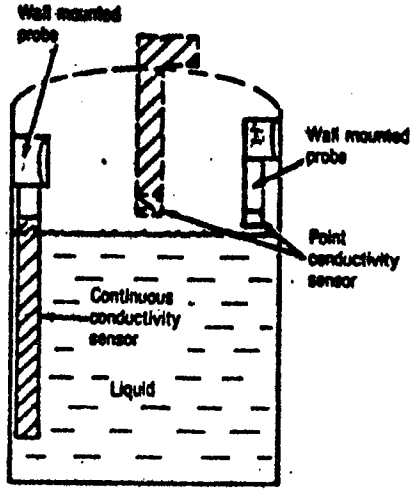

Conductivity level systems rely on the ability of a liquid to conduct an electric current. Source: Drexelbrook Engineering

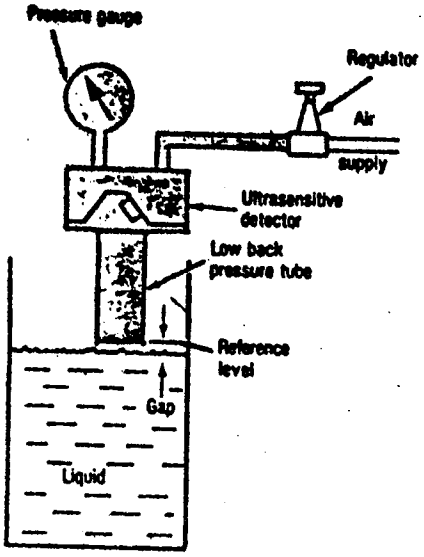

Ultra-sensitive back pressure sensor can measure level up to ±0.005 in. Source: Cutler Controls, Inc.

Fig. 29 Principles of liquid meters

Fig. 29 Principles of liquid level meters

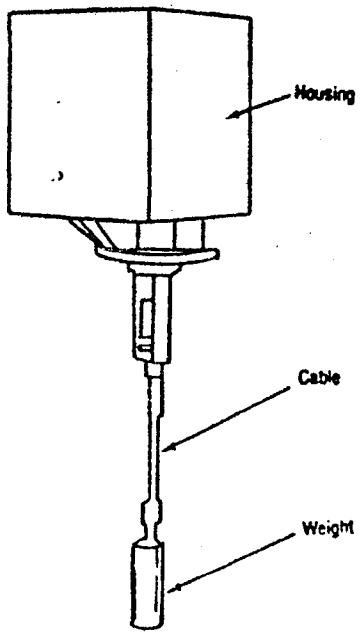

Weight and cable measures the level of bulk materials in silos and tanks. Source: Endress + Hauser.

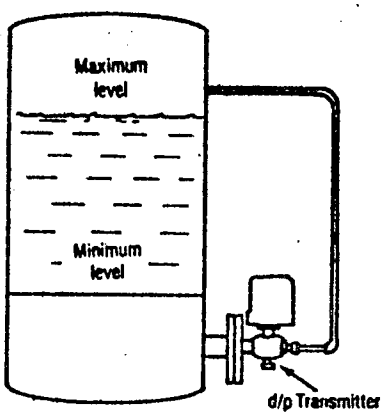

Differential pressure can be used to measure liquid level in open or closed tanks. Source: Foxboro Co.

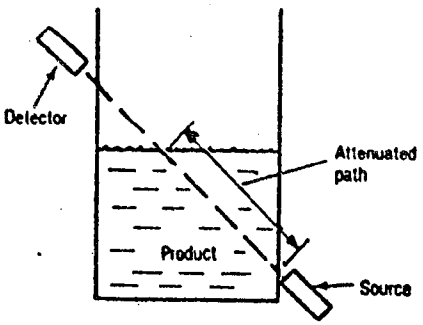

Nuclear radiation level devices provide point or continuous level measurements. Source: Nuclear Research

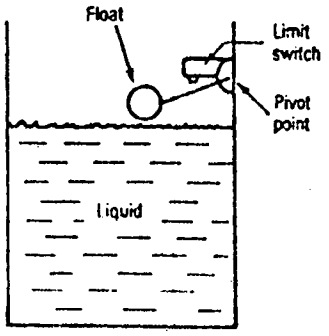

Float switch is a basic device for point level measurement of fluids.

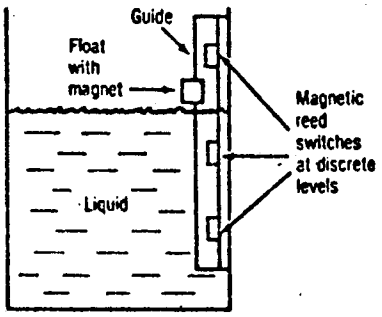

Float switch variation used for multiple level measurements.

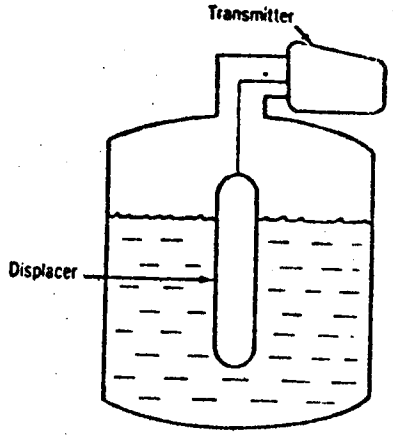

Displacer is partially immersed in the liquid. Its movement indicates level on a continuous basis. Source: Anderson

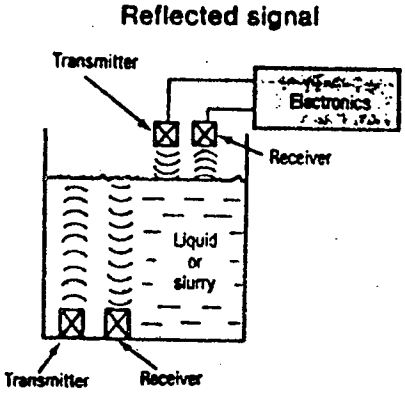

Ultrasonic and sonic level transducers can be mounted above or below surface. Transducer can have separate or combined transmitter and receiver.

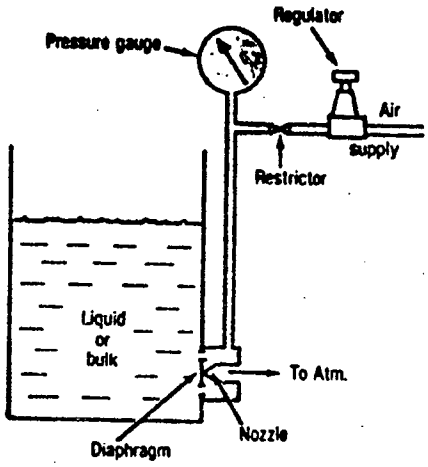

Force balance diaphragm can be used to measure level of liquids or granular solids.

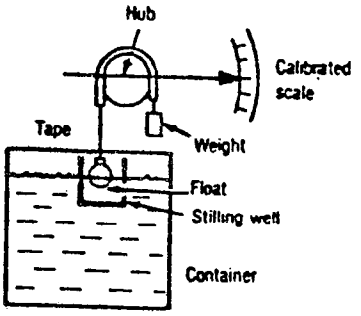

Float and tape provides a continuous measurement of liquid level in tanks. Source: Endress + Hauser, Inc.

2. Capacitance probes.
3. Impedance probes.

Current state of the art the development in void fraction measurement techniques are reviewed by Hewitt (1978)[21], Banerjee and Lahey (1981)[22]. Among these techniques, the neutron and ultrasonic beam methods are the most promising, since they can be applied to flow in high-pressure metallic pipes or high temperature liquid metal systems where other techniques based on electrical and optical principles cannot be used, i.e. non intrusive technique. The ultrasonic technique is also practical in large diameter pipes or vessels and for measurement of fast-transient phenomena, in contrast, radiation techniques are restricted to thin pipes and require a strong source and a large amount of radiation shielding to observe fast transient phenomena. Electrical methods have a potential advantage from an economical standpoint; however, they often interfere with the flow and change the two-phase phenomena, i.e. intrusive technique.

Capacitance, laser beam and ultrasonic methods are under development for liquid film thickness measurement, and the detailed method can be obtained in reference 23.

17.7.2 Acoustic Emission (AE)

The acoustic emission technique is based on the fact that the detection of the abnormal acoustic noise is generated from the fluid flow-component wall or pipe interactions. Difficulty with this method arises from the background, the electrical, the mechanical and the flow induced noises. Typical example of AE from the steam generator is shown in Figure 30. Detailed AE detection methods can be obtained from reference 24.

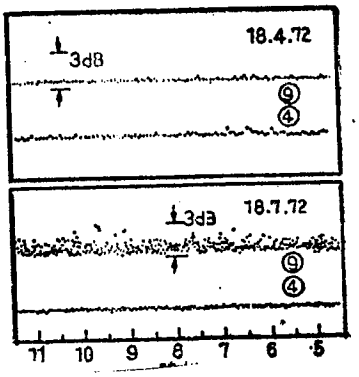

Figure 30: Example of AE signal in a PWR-steam generator (KWO reactor):
4) steam generator at normal operating condition
9) steam generator leading to plant shutdown after observing these noise levels (defect observed in SG).[25]

Copyright M.I.E.S. 1982

REFERENCES

1. "The Gradient Approach to Thermocouple Thermometry - R.J. Moffat, Measurement Systems Engineering", Stein Engineering Service Inc., 1977.

2. "Temperature Measurement Handbook", Omega Engineering, Inc., 1978.

3. "Measurement Systems: Application and Design", E.O. Doebelin, McGraw-Hill, 1966.

4. "A Survey of Temperature Measurement", J.R. Saltvold, AECL-5394, March 1976.

5. Rosemount Model 77 RTD Bulletin 1009, and Product Data SHeet 2001, Rosemount Inc., 1972.

6. BLH Pressure Transducers, Bulletin 402-4, BLH Electronics, 1973.

7. Kulite Semiconductor, Bulletin KPS-CQ3B, Kulite Semiconductor Products, Inc., 1974.

8. "Rosemount Model 1151 HP Alpaline Differential Pressure Transmitter for High Line Pressures", Product Data Sheet 2197, Rosemount Inc., 1973.

9. "Fluid Meters - Their Theory and Application, Sixth Edition 1971", (Errata 1974), ASME.

10. "An Evaluation of Existing Two-Phase Flow Correlations for use with ASME Sharp Edge Metering Orifices", L.T. Smith, J.W. Murdock, R.S. Applebaum, ASME Paper 76-WA/FM-3, 1976.

11. "Measurements of Vapour Quality and FLow Rate in Two-Phase Flow with Sharp Edged Circular Orifices", Z.H. Lin, Second Int. Symposium: Flow: Its Measurement and Control in Science and Industry, 1981.

12. "Measurement of Steam Quality in Two-Phase Upflow with Venturimeters and Orifice Plates", D.B. Collins, M. Gacesa, ASME Paper No. FE-6, 1970.

13. "A Model to Calculate Mass Flowrate and Other Quantities of Two-Phase Flow in a Pipe with a Densitometer, a Drag Disc, and a Turbinemeter", I. Aya, Oak Ridge National Lab. Report, ORNL/TM4759 (1975).

14. "Application of the Turbine Flowmeters in the Measurements of Steam Quality and Void", S.Z. Rouhani, Symp. In-Core Instrumentation, Oslo, 1974.

15. "Cross Section Averaged Density and Mass Flux Measurements in Two-Phase Flow Through Pipes", T.R. Heidrick, J.R. Saltrold, S. Banerjee and D. Nguyen, Measurements in Polyphase Flows, D.E. Stock, Ed., ASME Press, 1978.

Copyright M.I.E.S. 1982

16. "An Experimental Study of Flow Monitoring Instruments in Air-Water Two-Phase Downflow", J.D. Sheppard, P.H. Hayes and M.C. Wunn, Oak Ridge National Lab. Report, ORNL/TM .

17. "Ultrasonic Flowmeters", L.C. Lynnworth, Physical Acoustics, vol. 14, Academic Press.

18. "The Laser Doppler Anemometry", N. Nakatani, R. Yorisne and T. Yamada, Proc. ?? Dynamics Flow Conf., Marseilles and Baltimore, p. 583, DISA Electronic, Skovlunde, 1979.

19. "Laminar Fluid Flow Measurements Employing a White Light Fringe Image Velocimeter (WFIV)", J.H.C. Chan and E.A. Ballik, ASME J. Appl. Mech., 46, 218-220.

20. "A Look at Level Measurement Methods - Matching Applications with Devices", C.A. Belsterling, Instr. and Contr. Systems, 37-45, 1981.

21. "Measurement of Two-Phase Flow Parameters", G.F. Hewitt, Academic Press, London, 1978.

22. "Advances in Two-Phase Flow Instrumentation", S. Banerjee and R.T. Lahey, Jr., Adv. Nuclear Sci. and Tech., 13, 227-414.

23. "Flow Regime Characterization and Liquid Film Thickness Measurement in Horizontal Gas-Liquid Two-Phase Flow by an Ultrasonic Method", J.S. Chang, Y. Ichikawa and G.A. Irons, Measurements in Polyphase Flow - 1982, T.R. Hendrick and B.R. Patel, Eds., pp. 7-12, ASME Press, 1982.

24. "AE in PWR Power Plants", E.P. Ying, J. Acoustic Soc. Amer., 53, 1627, 1973.

25. "AE in KRB Power Plants", D.L. Parry, Exxon Nuclear Co., Report XN-310, 1975.

Copyright M.I.E.S. 1982